Techno-Economic Optimal Design of Solid Oxide Fuel Cell Systems for Micro-Combined Heat and Power Applications in the U.S.

Robert J. Braun

Division of Engineering,
Colorado School of Mines,
Golden, CO 80401

A techno-economic optimization study investigating optimal design and operating strategies of solid oxide fuel cell (SOFC) micro-combined heat and power (CHP) systems for application in U.S. residential dwellings is carried out through modeling and simulation of various anode-supported planar SOFC-based system configurations. Five different SOFC system designs operating from either methane or hydrogen fuels are evaluated in terms of their energetic and economic performances and their overall suitability for meeting residential thermal-to-electric ratios. Life-cycle cost models are developed and employed to generate optimization objective functions, which are utilized to explore the sensitivity of the life-cycle costs to various system designs and economic parameters and to select optimal system configurations and operating parameters for eventual application in single-family, detached residential homes in the U.S. The study compares the results against a baseline SOFC-CHP system that employs primarily external steam reforming of methane. The results of the study indicate that system configurations and operating parameter selections that enable minimum life-cycle cost while achieving maximum CHP-system efficiency are possible. Life-cycle cost reductions of over 30% and CHP efficiency improvements of nearly 20% from the baseline system are detailed.
[DOI: 10.1115/1.3211099]

Keywords: techno-economic, optimization, SOFC, micro-CHP, residential, energy systems design, combined heat and power, distributed generation, systems' analysis

1 Introduction

The accelerating development activity of solid oxide fuel cell technology has sparked interest in numerous power generation applications. The residential energy sector is one potential application for SOFCs and is responsible for nearly 22% of the total annual energy consumption in the U.S. [1] with over two-thirds of that energy consumption being used for low-efficiency space heating, domestic hot water, and air-conditioning [2]. While the residential sector has substantial room for improvements in energy efficiency, it is also one of the most challenging markets to compete in. Despite the efficiency advantages of high temperature fuel cell systems for onsite combined heat and power (CHP) generation, the application requirements of low maintenance, high durability (or lifetime), low cost, and high efficiency are severe. The increasing understanding of SOFC technology cost and performance enables a timely study of assessing optimal system configurations, parameter selection, and identification of key techno-economic parameters that will influence the success of SOFC-based micro-CHP systems in residential applications.

Fuel cell *system* performance characteristics are largely driven by cell-stack design parameters such as cell voltage, fuel utilization, operating temperature, and cathode gas temperature rise. Depending on where the fuel cell-stack is operated on its voltage-current characteristic, different proportions of electric and thermal outputs will be derived from the fuel cell system. Selection of fuel cell design parameters may either maximize power density or electric efficiency. The system design operating point strongly influences the capital costs of the major system hardware components, such as the SOFC stack, air blower, air preheater, and heat recovery equipment, and the operating costs, which are primarily associated with fuel consumption (or efficiency). The importance of techno-economic analyses, which utilize life-cycle costing, is the ability to quantify benefits of CHP operation and optimize a system design by judiciously taking into account the competing objectives of capital and operating cost minimization subject to the application constraints.

The objectives of the present work are to (1) quantitatively identify optimal SOFC system configurations for residential applications; (2) given an optimal configuration, select preferred operating parameters for the SOFC that minimize the life-cycle cost of the system; (3) quantify the importance of on-site cogeneration; and (4) establish the sensitivity of SOFC system cost-effectiveness to various economic parameters toward developing an understanding of the economic viability of SOFCs in the U.S. residential energy sector. Given the cost and complexity of stand-alone power systems, this analysis focuses on fuel cell systems for grid-connected, medium-sized ($\sim$200 m^2) single-family detached dwellings with access to pipeline natural gas. The analysis does not include potential environmental or economic benefits associated with emission reductions below that of conventional utility-supplied power and heat technologies. The study also employs U.S. national average utility energy pricing rather than focusing on a single geographic region or utility provider.

The body of work on residential-scale fuel cell-based micro-CHP systems is increasing, and much effort to date has proceeded assuming a single fuel cell system configuration. Previous work on techno-economic modeling and analysis of residential-scale fuel cell systems has focused largely on PEM-based systems [3–5]. Gunes and Ellis [4] presented an evaluation of a 4 kilowatt proton exchange membrane (PEM) fuel cell system with combined heat and power serving a residence. Their analysis focused

on an evaluation of grid-independent, fuel cell systems in terms of energetic, economic, and environmental variables. The study worked from a specific design and performance of the PEM fuel cell system. Khandkar et al. [6] developed a techno-economic model for a simple SOFC electric-only system at the 25 kW scale. This work generated design performance maps that measured the effect of capital cost and cost-of-electricity for variations in operating cell voltage and fuel utilization. Baratto et al. [7,8] examined the potential benefits of SOFC systems at the residential power scale but aimed toward truck auxiliary power unit applications and evaluated primarily in terms of a life-cycle assessment viewpoint. Hawkes and co-workers [9,10] performed studies on micro-SOFC-CHP systems for residential dwellings in the United Kingdom. In Ref. [9], their work focused on techno-economic modeling of a SOFC stack and power conditioning system for energy cost minimization. The model accounted for the SOFC stack, power conditioning, and supplemental boiler and was exercised to optimize operating and application strategies for United Kingdom residential loads, not system design. In Ref. [10], the authors explored the optimal size of a SOFC system and its sensitivity to changes in economic parameters such as net metering plans, fuel price, and component lifetimes. This study assumed a given simple SOFC-CHP system configuration and parameter settings. In an analogous manner, Alanne et al. [11] performed an assessment of micro-CHP residential systems using SOFCs for two different Canadian cities. Given a SOFC system configuration and operating characteristic, estimations regarding the sensitivity of SOFC economic sizing and competitiveness via payback analyses were made.

2 Methodology and Approach

Component and system models were developed that incorporate cost functions, which scale with both size and production volume. The detailed SOFC and balance-of-plant (BOP) models have been discussed elsewhere [12,13] and will only be briefly highlighted in Sec. 2.1. The basic approach is the integration of component cost functions with system models that predict SOFC-CHP energetic and economic performances. Of particular interest is the estimation of life-cycle costs that are influenced by first costs (capital, installation, etc.), operation and maintenance, fuel consumption, production volumes, system power rating, and by the choices of system configuration and SOFC operating parameters.

A comprehensive parametric optimization is carried out through a variation of system configurations and operating parameters, whereby optima are identified by the minimization or maximization of different life-cycle cost metrics. The optima are constrained by variable boundaries established from knowledge of residential application thermal and electrical energy requirements and practical SOFC operating parameters, such as operating temperature, voltage, fuel utilization, and fuel cell durability considerations.

A significant issue surrounding the use of fuel cells (and their efficiency) in residential applications is their ability to meet the highly noncoincident electric and thermal loads in either grid-connected or stand-alone configurations. That is, in either base load operation or electric load-following conditions, electricity and/or heat may be available when it is not needed or vice-versa. A key application parameter is the residential thermal-to-electric ratio (TER). The TER is the ratio of the thermal energy load or system output to the electrical demand. A TER may be based on space heating, space cooling, or domestic hot water demands within a residence, and its magnitude is highly dependent on location, building type, design, usage patterns, time of day, and time of year. The following design studies consider SOFC-based micro-CHP systems that produce TERs in the range 0.7–1.0 to be preferred for integration with residential domestic hot water systems [14]. The annual hourly averaged residential electric load is estimated at 1.0 kW, and the average domestic hot water load at 1.1 kW. Actual residential electricity demand can reach peak val-

ues of 9 kW or more over shorter time intervals (e.g., 15 min periods). The grid-connected system approach in this study assumes that dynamic loads are handled by the utility thereby enabling a focus on steady-state design and analysis of the fuel cell system. The fuel cell operating mode is considered to be base-loaded at a nominal power level near the annual hourly average of 1.0 kW. Given the hourly average electrical load, the prototypical residence used herein consumes 8760 kWh of electrical energy per year. The techno-economic model only employs average hourly loads and assumes an electric capacity factor of 90% for the fuel cell to account for both maintenance downtime and the inability of the SOFC to serve a large fraction of the dynamic loads. Details on techno-economic modeling are provided in Sec. 2.2.

2.1 SOFC System Modeling. The SOFC-CHP systems consist of pumping devices (blowers, ejectors, compressor, and water pump), gas-to-gas and gas-to-liquid heat exchangers, the fuel cell-stack, fuel processing hardware (desulfurizer and reformer), catalytic combustor, and power conditioning device. Component models capable of accurately predicting the performance of the fuel cell-stack, reformer, and remaining BOP hardware were implemented. The baseline system configuration is depicted in Fig. 1 and has been explored from thermodynamic viewpoints in a previous study [12]. A single-node (i.e., zero-dimensional) steady-state thermodynamic model is used for each of the system components with the exception of the solid oxide fuel cell-stack. Performance characteristics, such as blower and compressor efficiency, cell-stack voltage-current characteristics, and heat exchanger effectiveness, are included in the models. Air blower and fuel compressor isentropic efficiencies were set to 62.5% and 70%, respectively. The inverter was assumed to have an efficiency of 92% based on manufacturer's data [15]. These models were integrated and solved using a general-purpose equation solver [16] to determine all the state point variables in the system. More detailed descriptions of the models, validation, and parameter settings can be found in Refs. [12,13].

The net heat loss from high temperature components within the SOFC system to the surroundings constituents a significant fraction of the fuel energy input to the system. An estimate of the amount of thermal energy lost from the hot module to the ambient was carried out on a cylindrical vessel containing the cell-stack, air and fuel preheaters, and combustor. A vessel diameter (0.5 m) equal to twice the cell-stack height and a length of 0.6 m were used to estimate the heat transfer area. The temperature within the module was estimated by averaging the nominal cell-stack and the combustor temperatures. The overall *UA* of the vessel was found to be about 0.541 W/K using 5 cm of silica aerogel insulation with a thermal conductivity of 0.03 W/m K and resulted in an approximate heat loss equal to 9% of the fuel heating value input to the system [12]. Based on this estimate, the heat loss from the SOFC hot module to the ambient has been set to a value equal to 9% of the system fuel HHV energy input for each of the system configurations analyzed. The appropriateness of this setting was verified by observing that changes in the required vessel insulation thickness were less than 20% throughout the voltage-current operating envelope.

2.2 Cost Modeling. *Life-cycle costs.* The purpose of the cost modeling effort is to provide appropriate objective functions for optimal selection of system configuration and system design parameters. The cost model incorporates the latest available production cost forecasts for SOFCs and system components. The model makes use of component capital and maintenance costs, utility energy prices (grid electricity and natural gas), interest and energy inflation rates, and system efficiency. As the perspective on economic competiveness of residential-scale fuel cell systems is influenced in part on whether the owner of the system is the utility/energy service provider or the homeowner, two different life-cycle cost calculations were made: (1) the cost-of-electricity (COE) and
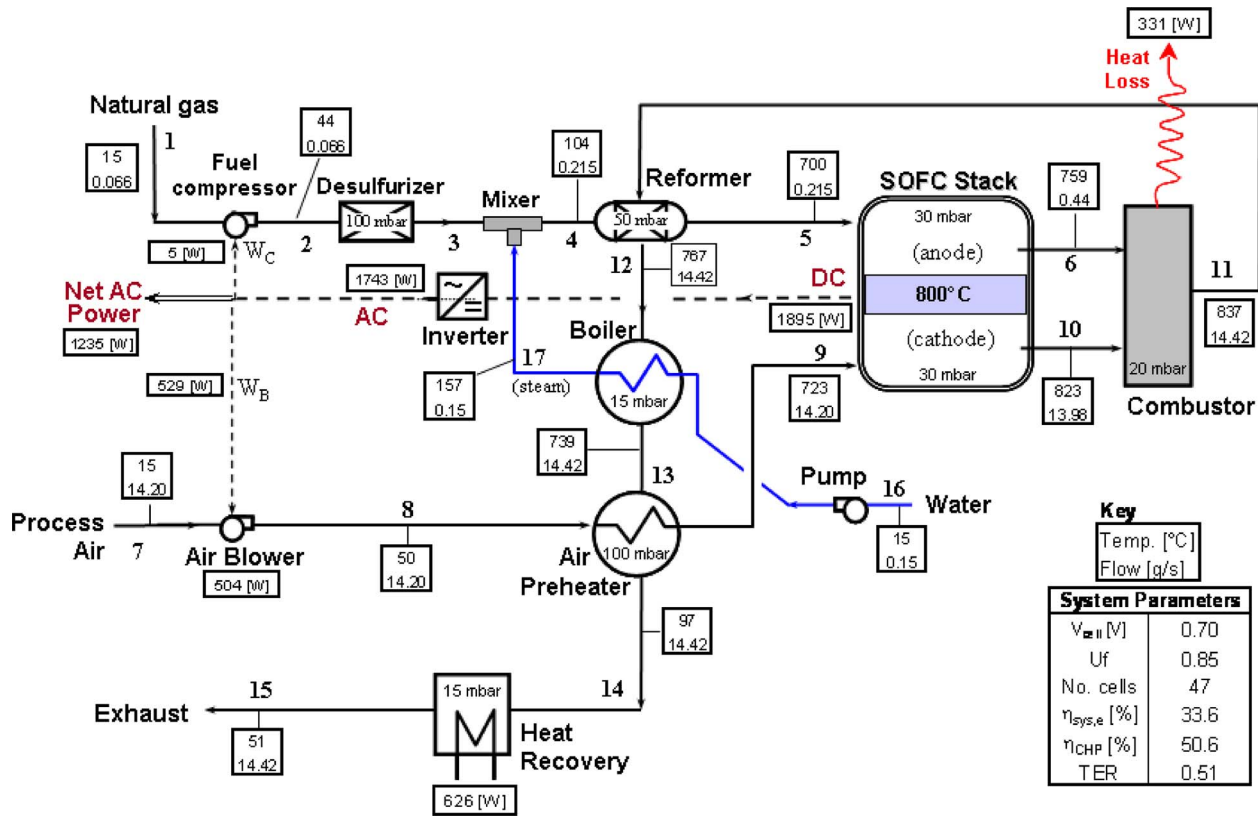
Fig. 1 Process flowsheet of methane-fueled SOFC-CHP system with external reforming (Case 2a)

(2) the life-cycle savings (LCS). Both COE and LCS functions may be based on either electric-only or CHP-systems where the value of the waste heat is accounted for.

In an electric-only application, the COE (expressed in US $/kWh) is written as

$$
\text{COE}_{\text{eo}} = \underbrace{k_1 \frac{R_F C_{\text{sys,eo}}}{\text{CF}_e \cdot A_{\text{plant}}}}_{\text{system capital cost}} + \underbrace{\sum_j \text{MC}_j}_{\text{maintenance}} + \underbrace{k_2 \frac{F_C}{\eta_{\text{sys},e}}}_{\text{fuel cost}} \qquad (1)
$$

where the first term in Eq. (1) is associated with the capital costs, the second term with maintenance costs, and the final term with fuel costs. In Eq. (1), R_F is the capital recovery factor, $C_{\text{sys,eo}}$ is the unit fuel cell system installed capital cost for electric-only systems in $/kW, CF_e is the system electric capacity factor, A_{plant} is the expected annual plant availability, MC_j is the levelized annual maintenance cost of component j in $/kWh, F_c is the unit fuel cost in $/therm, $\eta_{\text{sys},e}$ is the fuel cell system electric efficiency (higher heating value basis), and k_1 and k_2 are unit conversion constants. The levelized annual maintenance cost for each component j was estimated by determining the present worth of all replacement costs over the life of the power plant as follows:

$$
\text{MC}_j = \frac{R_F C_j \left[\dfrac{(1+i_{\text{infl}})^{n_1}}{(1+i)^{n_1}} + \dfrac{(1+i_{\text{infl}})^{n_2}}{(1+i)^{n_2}} + \cdots \right]}{\text{CF}_e \cdot A_{\text{plant}} \cdot 8760} \qquad (2)
$$

where the numerator in Eq. (2) represents the present worth of annual payments for the replacement cost of component j replaced in years $n_1, n_2, \ldots$ utilizing an equipment cost inflation rate i_{infl} and an interest rate i. Levelized maintenance costs were estimated by amortizing each of the expected service requirements over the life of the system. The SOFC stacks are assumed to have an operational life of 5 years (40,000 h) with a salvage value of 10% of the original investment. These considerations translate into a replacement of the entire fuel cell-stack two times during the 15

year plant life. The catalysts in the steam reformer and combustor are assumed to be replaced every 5 years (40,000 h) and the desulfurizer sorbent bed is replaced annually.

In a CHP-system, the net cost-of-electricity must be offset by the amount of thermal energy recovered and utilized for either space or hot water heating. Ellis and Gunes [17] showed the COE for the CHP case to be determined by

$$
\text{COE}_{\text{CHP}} = \underbrace{k_1 \cdot \frac{R_F \cdot C_{\text{sys,CHP}}}{\text{CF}_e}}_{\text{capital and maintenance cost}} + \underbrace{k_1 \cdot \frac{C_{\text{maint,CHP}}}{\text{CF}_e}}_{\text{system maintenance}} + \underbrace{k_2 \cdot \frac{F_c}{\eta_{\text{sys},e}}}_{\text{fuel cost}}
$$
$$
- \underbrace{k_2 \cdot \frac{F_{\text{th}} \cdot \varepsilon_H \cdot F_c}{\eta_{\text{sys},e} \cdot \eta_{\text{htg}}}}_{\text{thermal energy credit}} \qquad (3)
$$

where $C_{\text{sys,CHP}}$ is the unit fuel cell system installed cost for co-generation systems in $/kW, $C_{\text{maint,CHP}}$ is the maintenance cost, ε_H is the heating or thermal energy recovery efficiency, F_{th} is the fraction of thermal energy from the fuel cell system that can be used, η_{htg} is the efficiency of the heating system that is displaced by the exported thermal energy from the fuel cell system, and k_1 and k_2 are unit conversion constants. CF_e is defined as the kWh of electricity produced divided by the product of the rated capacity of the system and 8760 h/year. The product of F_{th} and ε_H is the net thermal energy conversion efficiency and is equivalent to $(\eta_{\text{CHP}} - \eta_{\text{sys},e})$, where η_{CHP} is the system cogeneration efficiency. Transmission and distribution costs do not factor into the cost-of-electricity for on-site power generation. Employing a levelized maintenance cost and a heating capacity factor that accounts for situations where the heat that is available from the fuel cell system is not utilized, Eq. (3) is rewritten as

$$\mathrm{COE_{CHP}} = \underbrace{k_1 \frac{R_F C_{\mathrm{sys,CHP}}}{CF_e}}_{\text{system capital cost}} + \underbrace{\sum_j \mathrm{MC}_j}_{\text{levelized system maintenance}}$$

$$+ \underbrace{k_2 \frac{F_C}{\eta_{\mathrm{sys},e}} \cdot \left[1 - \frac{(\eta_{\mathrm{CHP}} - \eta_{\mathrm{sys},e})}{\eta_{\mathrm{htg}}} \cdot CF_h \right]}_{\text{fuel cost-thermal energy credit}} \qquad (4)$$

where CF_h is the annual average CHP-system heating capacity factor defined here as

$$CF_h = \frac{\dot{Q}_{\mathrm{HR}}}{\dot{Q}_{\mathrm{load,avg}}} \cdot CF_e \cdot A_{\mathrm{plant}} \qquad (5)$$

In Eq. (5), $\dot{Q}_{\mathrm{HR}}$ is the amount of heat recovered from the fuel cell system at design conditions in kilowatt and $\dot{Q}_{\mathrm{load,avg}}$ is the average hourly residential thermal load (in this case, domestic hot water) in kilowatt. On an annual basis, the value of CF_h must be less than 1.

The life-cycle savings are computed from the difference between life-cycle cost estimates of the utility/energy provider services and the life-cycle costs of a solid oxide fuel cell system. That is,

$$\mathrm{LCS_{SOFC}} = \mathrm{LCC_{utility}} - \mathrm{LCC_{SOFC}} \qquad (6)$$

The individual life-cycle cost terms (e.g., $\mathrm{LCC_{SOFC}}$) are calculated by adapting the $P_1 - P_2$ method presented by Duffie and Beckman [18] for the case of grid-connected fuel cell power systems that may not supply 100% of the electricity and/or thermal energy requirements of a residence. In the $P_1 - P_2$ method, the life-cycle cost is considered to be the sum of two terms ($\mathrm{LCC} = P_1 F + P_2 C$) that are proportional to the first year operating cost (F) and to the installed capital costs (C) of the system. The life-cycle cost of a SOFC power system is determined from

$$\mathrm{LCC_{SOFC},\it j} = P_1(F_{\mathrm{SOFC},j} + F_{\mathrm{utility,ngas}}) + P_2 C_{\mathrm{sys},j} \dot{W}_{\mathrm{sys,net}}$$
$$+ P_3 F_{\mathrm{utility,elec}}(1 - CF_e A_{\mathrm{plant}}) \qquad (7)$$

where the subscript j refers to either an electric-only or a CHP type system, F_{SOFC} is the annual fuel cost to operate the SOFC system, $F_{\mathrm{utility,ngas}}$ is the annual natural gas fuel cost the utility charges to serve the thermal energy demand in the home, $\dot{W}_{\mathrm{sys,net}}$ is the rated power capacity of the SOFC system, and $F_{\mathrm{utility,elec}}(1 - CF_e A_{\mathrm{plant}})$ is the net grid electricity cost to deliver power to the home that is not met by the fuel cell system. The constants P_1 and P_3 are present worth factors that depend primarily on the number of years that the equipment is expected to operate, the inflation rate for expenses related to operation (typically the rate at which the cost of the fuel or electricity inflates), and the market discount rate. The constant of proportionality P_2 depends on many economic parameters, including the down payment on the first costs (capital and installation), the mortgage interest rate, the market discount rate, the term of the economic analysis, the salvage value of the equipment at the end of economic analysis period, and other economic factors related to first costs such as tax credits, property tax, maintenance, and depreciation. It is also important to note that the life-cycle cost employed in this analysis does not include any benefit of selling fuel cell-produced electricity back to the grid via a net metering plan. Such benefits are not cost-effective for the combined heat and power system owner when the total electricity produced exceeds the consumption over a billing cycle due to utility buyback rates that are typically lower than the cost of the natural gas supplied to the fuel cell system [19,20].

In a conventional system, residential electrical energy and hot water demands are typically served with a gas-fired water heater and grid-supplied electricity. The life-cycle costs of the utility are determined from the relation

$$\mathrm{LCC_{utility}} = P_1 F_{\mathrm{utility,ngas}} + P_3 F_{\mathrm{utility,elec}} \qquad (8)$$

The annual energy costs (F) in Eqs. (7) and (8) are calculated from

$$F_{\mathrm{SOFC},j} = \frac{8760 k_2 F_C \dot{W}_{\mathrm{sys,net}} CF_e A_{\mathrm{plant}}}{\eta_{\mathrm{sys},e}} \qquad (9)$$

$$F_{\mathrm{utility,ngas}} = \frac{8760 k_2 F_C (\dot{Q}_{\mathrm{load,avg}} - \dot{Q}_{\mathrm{HR}} CF_e A_{\mathrm{plant}})}{\eta_{\mathrm{htg}}} \qquad (10)$$

$$F_{\mathrm{utility,elec}} = 8760 \dot{E}_{\mathrm{elec,avg}} P_{\mathrm{elec}} \qquad (11)$$

where in Eq. (10) the product term $\dot{Q}_{\mathrm{HR}} CF_e A_{\mathrm{plant}}$ is zero for the $\mathrm{LCC_{utility}}$ calculation, and $\dot{E}_{\mathrm{elec,avg}}$ in Eq. (11) is the annual hourly average electric load in kW and P_{elec} is the annual average electricity price in \$/kWh.

Hydrogen fuel cost is estimated at \$3.30/kg H_2 per a U.S. Department of Energy study [21]. The cost of hydrogen was based on steam methane reforming of natural gas with pressure swing adsorption and a national average industrial natural gas price of \$0.0113/kWh. Residential natural gas prices for powering the micro-CHP SOFC system vary significantly with geographic location, and the base case is established at \$1.00/therm or \$0.03412/kWh. The utility price for electricity also varies significantly across the U.S. and the national average of \$0.104/kWh in 2006 [22] was employed for the base case. The sensitivity of the results to variations in utility pricing is explored in this study.

Capital equipment costing. Component capital costs are dependent on both the production volume and capacity (or size) of the hardware. In order to test the sensitivity of the life-cycle costs to these variables, the cost model equations were formulated to be inclusive of both the economy of production and economy of scale. The basic formulation for estimating the cost of component i at production volume V is given as

$$C_{i,V} = C_{i,V_{\mathrm{ref}}}^{\mathrm{ref}} \cdot \left(\frac{V}{V_{\mathrm{prod}}^{\mathrm{ref}}} \right)^k \cdot \left(\frac{S}{S_i^{\mathrm{ref}}} \right)^y \qquad (12)$$

where $C_{i,V_{\mathrm{ref}}}^{\mathrm{ref}}$ is the reference cost for component i at some reference production volume $V_{\mathrm{prod}}^{\mathrm{ref}}$ and known equipment size S_i^{ref}, and k and y are volume production and equipment size scaling parameters, respectively. The value of k has been assumed to be the same for all components in the system and was estimated at -0.1365 using data regression of system cost estimates by Mugerwa and Blomen [23] for different manufacturing volumes of molten carbonate and phosphoric acid fuel cell systems.

The bulk of the component costing is derived from studies by Arthur D. Little (ADL) [24] and Thijssen [25] on 5 kW SOFC-based auxiliary power units (APUs). Others have also presented cost studies [26–29] for fuel cell systems; however, the 2001 ADL and 2007 Thijssen studies remain as the most comprehensive for planar SOFC power systems at this scale. The SOFC stack manufacturing costs utilized herein are based on anode-supported planar cells with metallic interconnects. The reference unit cell design is comprised of a Ni/Zr cermet anode (700 μm thick), an yttria-stabilized zirconia (YSZ) electrolyte (10 μm), a strontium-doped lanthanum manganite (LSM) cathode (50 μm), and a metallic interconnect. The interconnect material is dependent on the cell operating temperature and is either a high temperature stainless steel ($\leq 700°C$), a superalloy metal ($700 - 900°C$), or a La Chromite ceramic ($> 900°C$). The area specific cost of the complete cell-stack module consisting of repeat unit cells (electrode-electrolyte-interconnect assembly) and balance of stack components (compression, seals, manifolds, etc.) was estimated at about \$472/m^2 for production volumes of 500,000 stacks/year [24]. However, this cost is based on stainless steel interconnect materials, which is not considered sufficiently robust for stationary

Table 1 System component capital cost data summary

Item	Component	Cost equation[a]	Baseline system unit costs[a,b] ($/kW)
1	SOFC hardware[c]	$C_1 = 1774.9 \cdot (V_{prod})^{-0.1365} \cdot F_{T_{cell}} \cdot A_{e,stack} \cdot (\dot{W}_{sys,net})^{-1}$	490
2	Fuel compressor	$C_2 = 58.55 \cdot (V_{prod})^{-0.1365}$	34
3	Desulfurizer	$C_3 = 135.71 \cdot (V_{prod})^{-0.1365} \cdot (\dot{m}_{fuel}[kg/h])^{0.67} \cdot (\dot{W}_{sys,net})^{-1}$	25
4	Steam reformer	$C_4 = \dfrac{729.76}{\dot{W}_{sys,net}} \cdot (V_{prod})^{-0.1365} \cdot (\dot{m}_{fuel}[kg/h])^{0.67} \sqrt{\xi}$	132
5	Boiler+pump	$C_5 = [108.75 \cdot (V_{prod})^{-0.1365} + 63.025] \cdot \dfrac{(\dot{Q}_{steam}[kW])^{0.67}}{\dot{W}_{sys,net}}$	55
6	Anode ejector	$C_6 = 32.732 \cdot (V_{prod})^{-0.1365} \cdot (\dot{m}_{fuel}[kg/h])^{0.67} \cdot (\dot{W}_{sys,net})^{-1}$	–
7	Cathode air blower+air filter	$C_7 = [413.25 \cdot (V_{prod})^{-0.1365} + 16.23] \cdot \dfrac{(\dot{W}_{blower}[kW])^{0.807}}{\dot{W}_{sys,net}}$	120
8	Air preheater	$C_8 = 4.4403 \cdot (V_{prod})^{-0.1365} \cdot (UA[W/K])^{0.67} \cdot (\dot{W}_{sys,net})^{-1}$	234
9	Cathode ejector	$C_9 = 45.59 \cdot (V_{prod})^{-0.1365}(\dot{m}_{cath,recycl}[g/s])^{0.67} \cdot (\dot{W}_{sys,net})^{-1}$	–
10	Cathode recycle blower	$C_{10} = \dfrac{599.22}{\dot{W}_{sys,net}} \cdot (V_{prod})^{-0.1365} \cdot (\dot{m}_{cath,recycl}[g/s])^{0.807}$	–
11	Catalytic combustor	$C_{11} = \dfrac{1.4207}{\dot{W}_{sys,net}} \cdot (V_{prod})^{-0.1365} \cdot (\dot{m}_{exhgas}[kg/h])^{0.82}$	17
12	Hot water tank (225ℓ)	$C_{12} = 859.52 \cdot (V_{prod})^{-0.1365} \cdot (\dot{W}_{sys,net})^{-1}$	408
13	Power conditioning	$C_{13} = 487.72 \cdot (V_{prod})^{-0.1365} \cdot (\dot{W}_{sys,net}[kW])^{-0.22}$	273
14	Miscellaneous BOP[d]	$C_{14} = 621.45 \cdot (V_{prod})^{-0.1365} \cdot (\dot{W}_{sys,net}[kW])^{-0.829}$	306
15	Fabrication/assembly (indirect)	$C_{15} = 0.088 \cdot \left(\sum_{i=1}^{k} C_i\right)$ where k varies with system	124
16	Installation	$C_{16} = 300 / \dot{W}_{sys,net}$	243

[a]2006 USD.
[b]1.235 kW net ac power system at production volume of 50,000 units/year.
[c]Per m^2 of the electroactive area at 800°C.
[d]Includes startup burner, N$_2$ purge system, piping, valves, wiring, sensors, and non-SOFC stack insulation.

SOFC fuel cell systems whose life requirement is substantially longer than APU-based systems and where the average cell temperature is expected to be greater than 700°C. Therefore the cost of the fuel cell-stack was increased by a net of 40% over the ADL value for operating temperatures above 700°C, but less than 850°C, by taking into account cost factor increases associated with a Haynes 230-class interconnect [30] and the percentage of total stack cost that is associated with the interconnect itself [25]. For operation above 850°C, the cost was increased by 80% of the ADL value for utilization of a ceramic interconnect. The physical cell area is 100 cm^2 and the cell electroactive area is 81 cm^2 with a cell pitch of 2 cells/cm.

The fuel processing hardware is dependent on the system configuration and may include a fuel compressor, a desulfurizer (sorbent bed), a catalytic steam reformer (CSR) with integral fuel preheater, a mixer/ejector, and either an anode recycle device or a steam boiler and water pump (see Fig. 1). The CSR reference cost was based on a 2002 study by TIAX [31] and the capital cost of the CSR was made dependent on the amount of conversion in the reformer and the mass flow of fuel gas to be reformed. The cost equation is modified from general equation (12) slightly to account for the extent of conversion (ξ) in the reformer

$$C_{CSR,V} = C_{CSR,V_{ref}}^{ref} \cdot \left(\frac{V}{500,000}\right)^{-0.1365} \cdot \left(\frac{\dot{m}_{fuel}}{\dot{m}_{fuel}^{ref}}\right)^{0.67} \cdot \sqrt{\xi} \quad (13)$$

where ξ varies between 0.1 and 1.0 and is set to 0.1 for conversions less than 0.1 (i.e., for internal reforming (IR) >90%).

The cost scaling exponent of 0.67 in Eq. (13) is determined from nonlinear regression of fuel processing cost data as a function of system power output presented by Lundberg [26] for commercial-scale (from 50 kW to 1 MW) stationary SOFC sys-

tems fueled from natural gas. The component unit costs for the baseline system configuration of Fig. 1 are provided in Table 1 along with a summary of the general component cost equations formulations.

Centrifugal air blower types are often used in fuel cell applications and given the low flow, high pressure rise requirement, off-the-shelf blowers are not typically available. However, due to the numerous demonstration systems, cathode blower costs are becoming well-established and have been estimated at $120/kW of net system power for the baseline system configuration. Cathode recycle blowers are presently in the design and development stage and are not yet available due to their high temperature service requirements. Nevertheless, the cost of recycle blower technology is continuously being explored (e.g., via the DOE SECA program) and has been estimated at three times the centrifugal air blower cost [32]. Air filter cost is considered as fixed at $10/kW. Fuel compressor, desulfurizer, anode and cathode ejectors, air preheater, and catalytic combustor costing are also derived from the ADL study. The desulfurizer cost estimate is based on low-temperature sorbent bed technology. Air preheater cost estimates in Ref. [24] are based on high temperature stainless steels. However, as the use of a superalloy, such as Haynes 230, is anticipated for most systems where long life at elevated temperature is required this cost has been increased by an effective cost factor of 2.8 [30].

The hot water storage tank was sized at 60 gal (225 l) based on a previous study of peak hourly tank water temperatures for prototypical household water demand over the course of 8760 h [13]. The tank cost estimate was linearly scaled from 75 gal (300 l) tank cost data [33]. Power conditioning costs were generated by utilizing the DOE unit cost target of $150/kW at 500,000 unit produc-

tion volumes and scaling down to 50,000 units/year production levels. Miscellaneous balance-of-plant and fabrication and assembly cost estimates were taken from the ADL study [24] and installation costs were assumed fixed at $300 (~25% of system capital cost) and do not include grid-connection fees.

The total capital cost of the system is determined by summing each of the component contributions

$$C_{\text{sys,total}} = \sum_{1}^{N} C_j \quad (14)$$

The capital cost model estimates a system unit cost of $2268/kW for the CHP-system with hot water production shown in Fig. 1, and a cost of $1860/kW for an electric-only version (no heat recovery hardware) of the baseline system configuration.

Cost model benchmarking. Significant uncertainty exists in estimating equipment and system costs, especially for small capacities as required for residential-scale systems. Factors, such as component size and availability, raw material price volatility, hardware technology status, purchase volumes, and service life and temperature requirements will affect hardware cost estimates. Nevertheless, system cost estimates that take into account economies of scale and production can be made to within about ±30% of the actual system cost. Despite the large uncertainties in system cost estimates, the utility of this type of analysis lies in the *relative* changes in capital and operating costs due to changes in system design configurations, operating parameters, and application operating strategies. Uncertainty in the *relative* economic change between system configurations is estimated at 5–10%.

Cost predictions for the SOFC system were compared against literature data and found to be within 5–10%. For SOFC systems in the 3–10 kW-class, DOE SECA teams have reported system unit capital costs ranging from $741/kW to $774/kW for production volumes of 50,000 units/year [34,35]. These units do not include ac inverters and heat recovery hardware. The cost model utilized in this study predicts a system capital cost of $815/kW for a comparable 5 kW SOFC system operating at a power density of 0.4 W/cm².

2.3 Performance Definitions. SOFC cell-stack efficiency, net system electric efficiency, and system cogeneration efficiency used throughout the present work are defined as

$$\eta_{\text{SOFC}} = \frac{\dot{W}_{\text{dc}}}{(\dot{n}_{\text{fuel,in}} \cdot \text{HHV}_{\text{fuel}})_{\text{inlet}}^{\text{anode}}} \quad (15)$$

$$\eta_{\text{sys},e} = \frac{\dot{W}_{\text{ac,net}}}{(\dot{n}_{\text{fuel,in}} \cdot \text{HHV}_{\text{fuel}})_{\text{inlet}}^{\text{system}}} \quad (16)$$

$$\eta_{\text{CHP}} = \frac{\dot{W}_{\text{ac,net}} + \dot{Q}_{\text{HR}}}{(\dot{n}_{\text{fuel,in}} \cdot \text{HHV}_{\text{fuel}})_{\text{inlet}}^{\text{system}}} \quad (17)$$

where $\dot{W}_{\text{dc}}$ is the stack dc power developed, $\dot{W}_{\text{ac,net}}$ is the net system ac power, $\dot{Q}_{\text{HR}}$ is the amount of thermal energy from the SOFC system exhaust gas converted to low-grade (60°C) hot water, $\dot{n}_{\text{fuel,in}}$ is the molar system fuel flow rate, and HHV_{fuel} is the fuel higher heating value.

The *in-cell* fuel utilization refers to the amount of fuel electrochemically oxidized in the anode compartment of the cell-stack. When anode gas recycle (AGR) is used, the *system* fuel utilization is evaluated at the system fuel input boundary and is different in magnitude than the in-cell utilization. Both utilizations are defined as follows where $\dot{n}_j$ refers to the molar flow rate of the species of interest:

$$U_{f,\text{cell}} = \frac{(\dot{n}_{\text{H}_2,\text{consumed}})}{(4\dot{n}_{\text{CH}_4} + \dot{n}_{\text{H}_2} + \dot{n}_{\text{CO}})_{\text{inlet}}^{\text{anode}}}, \quad U_{f,\text{sys}} = \frac{(\dot{n}_{\text{H}_2,\text{consumed}})}{(4\dot{n}_{\text{CH}_4})_{\text{feed}}^{\text{system}}}$$

$$(18)$$

The amount of stoichiometric air for hydrogen- and methane-fueled systems is calculated using the following respective relations:

$$\lambda_{\text{air}}|_{\text{CH}_4} = \frac{\dot{n}_{\text{O}_2,\text{sys}}}{2\dot{n}_{\text{CH}_4,\text{sys}}}, \quad \lambda_{\text{air}}|_{\text{H}_2} = \frac{2\dot{n}_{\text{O}_2,\text{sys}}}{\dot{n}_{\text{H}_2,\text{sys}}} \quad (19)$$

where the molar flow rates in Eq. (19) are taken at the system feed to the plant. The total airflow to the system is significantly greater than the stoichiometric requirements and is determined via energy balances that include the magnitude of the cell polarizations, the amount of internal reforming, and the allowable air temperature rise in the cathode.

3 Optimization Study of SOFC-CHP System Configurations

The integrated thermo-economic system models are used in a parametric optimization study to (1) identify a residential-scale SOFC-CHP system concept that offers the lowest life-cycle costs, (2) select optimal SOFC operating parameters for the identified system configuration, and (3) evaluate life-cycle cost sensitivities to a variation in economic parameters. The system configurations investigated focus on concepts related to reactant gas processing via external and internal reformings of methane (natural gas), as well as anode and cathode gas recirculations. The impact of fuel type (hydrogen versus natural gas) on system life-cycle cost is also examined.

Five different system configurations are explored and are denoted as follows: Case (1) hydrogen-fueled, Case (2) methane-fueled with waste heat boiler, Case (3) methane-fueled with cathode gas recycle (CGR) and waste heat boiler, Case (4) methane-fueled with AGR, and Case (5) integration of CGR, AGR, and IR concepts. The analyses are carried out for a system that produces a fixed net ac power output of 1.235 kW when operating a SOFC stack at a nominal temperature of 800°C, an average cell voltage of 0.7 V/cell, a design cathode air temperature rise, ΔT_{air}, of 100°C, and a system fuel utilization of 85%. The SOFC power output was selected so that a system annual average electric capacity factor of 90% could be obtained over the 5 year life of the SOFC stack.

Detailed energetic and technical performance evaluations of the system configurations in Cases 1–5 have been reported previously [12]. They are briefly reviewed here for the case of a specified net power of 1.235 kW to complement the subsequent life-cycle cost discussion. A process and performance description for hydrogen-fueled systems (Case 1) is first presented followed by the methane-fueled system configurations beginning with the baseline system (Case 2a). Process flowsheets are provided in Figs. 1–3, and a summary of key performance parameters is given in Table 2.

3.1 Hydrogen-Fueled SOFC-CHP System Description. Figure 2 depicts a process flow diagram for a conceptual hydrogen-fueled SOFC system operating near atmospheric pressure with heat recovery (Case 1a) and cathode gas recycle (Case 1b). Process flow data with component pressure drop data for Case 1b are also included in this figure. Depending on the method of hydrogen production, delivery, and storage, the system may not require a fuel-side compressor, but one is assumed in this configuration. A low-pressure hydrogen-rich fuel mixture (97% H_2 and 3% H_2O) at 15°C enters the system and is compressed and preheated to 700°C before admittance to the cell-stack assembly, which operates at a nominal temperature of 800°C. Air with a stoichiometric ratio of 11 enters at station 5 and is preheated to
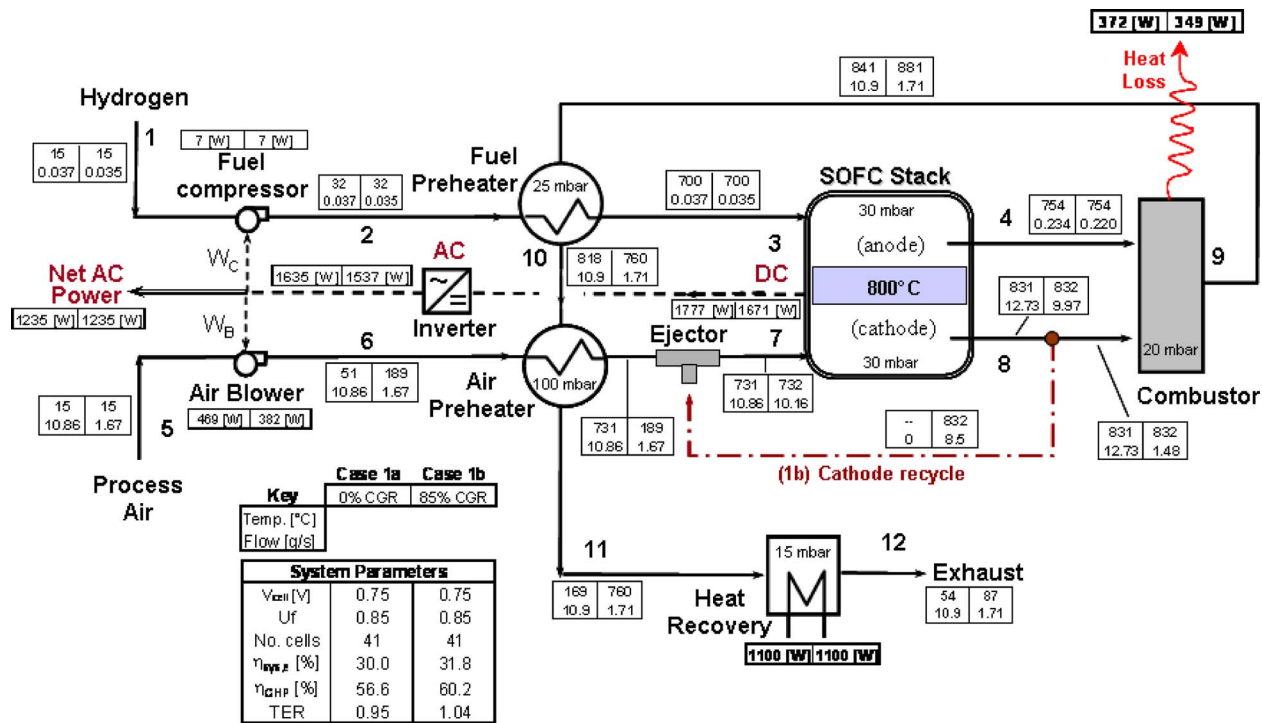
Fig. 2 Process flowsheet of hydrogen-fueled SOFC-CHP system (Case 1a) and with CGR (Case 1b)

731°C before delivery to the cathode compartment of the cell-stack. The SOFC module contains a 41-cell stack operating at 0.75 V/cell that produces 1.78 kW of dc power, which is inverted to ac. After parasitic power consumption by the air blower and fuel compressor, 1.235 kW net ac is generated by the system for an overall HHV efficiency of 30.0% (35.5%-LHV). Depleted anode gas products exit the stack and catalytically combust using cathode exhaust to obtain a temperature of 841°C. The product

gas stream is cooled to just above 169°C by reactant preheat duties. The remaining thermal energy content of the product gas is used to heat water from a temperature of 15°C to less than 60°C in a heat recovery heat exchanger that functionally serves as a water preheat tank. Approximately 1.2 kW of low-grade heat in the form of domestic hot water could be recovered from the product gas. However, given that the average domestic hot water load is 1.1 kW, only this amount can be utilized. The system exhausts
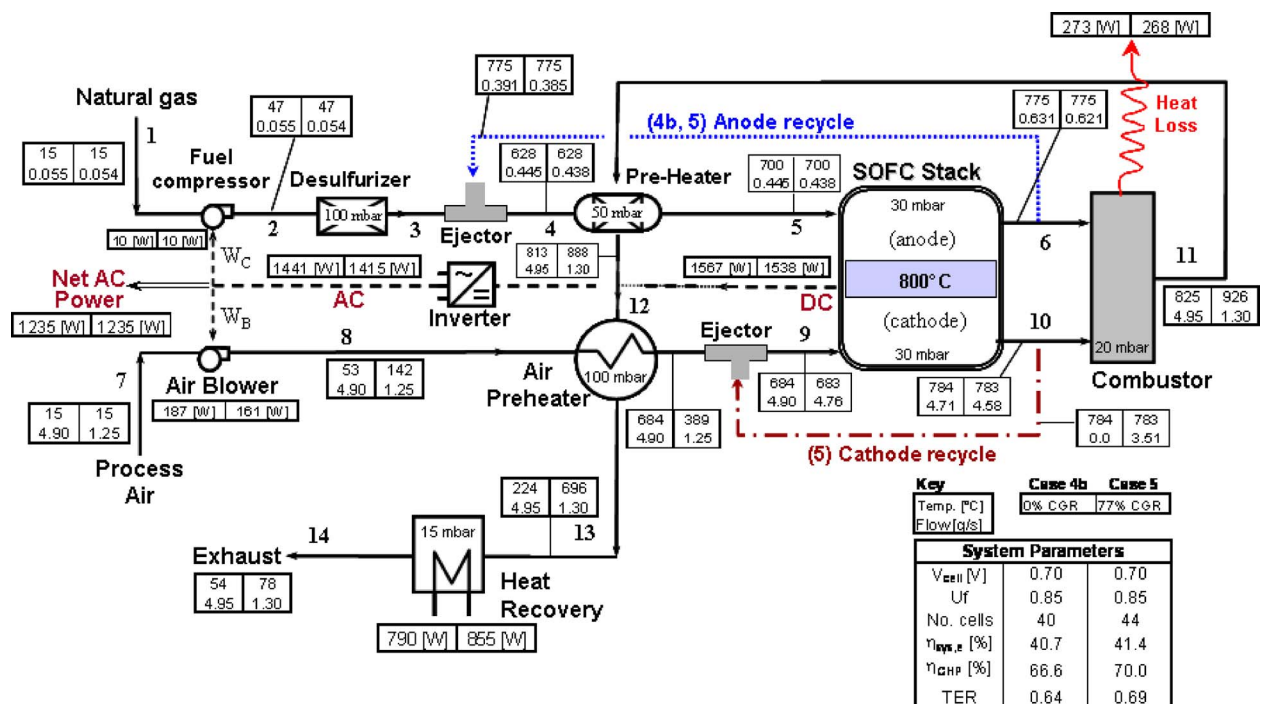
Fig. 3 Process flowsheet of CH₄-fueled SOFC-CHP system with IR and tail gas recycle (Cases 4b and 5)

Table 2 Performance comparison for 1.235 kW net ac power at a nominal 0.7 V/cell design point

System concept	Air ratio λ_{air}	Air blower power (W)	Air preheater UA (W/K)	TER (W_{th}/W_e)	Heat loss (W)	Power density (W/cm^2)	System electric efficiency (%-HHV)	CHP efficiency (%-HHV)
(1a) H$_2$-fueled	10.9	469	78.3	0.95	372	0.441[a]	30.0	56.6
(1b) H$_2$-fueled cathode recycle	1.8	382	0.0	1.04	349	0.407[a]	31.8	60.2
(2a) Base Case 0% IR with boiler	12.5	504	180.6	0.51	331	0.407	33.6	50.6
(2b) 100% IR with boiler	5.7	188	29.8	0.36	271	0.388	41.1	55.9
(3a) 0% IR with cathode recycle	2.3	402	0.65	0.65	311	0.386	35.7	58.9
(3b) 100% IR with cathode recycle	1.1	157	0.21	0.46	265	0.347	41.6	60.7
(4a) 0% IR with anode recycle	12.7	581	170.8	1.0	349	0.417	31.8	60.2
(4b) 100% IR with anode recycle	5.2	187	22.2	0.65	273	0.389	40.7	66.6
(5) 100% IR with AGR/CGR	1.4	161	0.61	0.69	268	0.350	41.4	70.0

[a]The cell design point voltage for H$_2$-fueled system is 0.75 V/cell.

to the atmosphere at a temperature near 54°C for an overall cogeneration efficiency of 56.6% (67.2%-LHV).

Cathode gas recycle is incorporated via an ejector operating at 20% efficiency[1] in Case 1b. The pressure drop in the recycle loop is 30 mbars, which, when coupled with the ejector efficiency operating point, sets the primary driving pressure required at the ejector inlet. Approximately 85% by mass of the cathode exhaust is recirculated, which reduces stack power density by about 10% and eliminates the air preheater duty (an air preheater of some capacity is likely during system startup) and the associated pressure drop with this component. Overall, there is a reduction of 85% in system air input and a net reduction of about 18% in the blower power requirement. Net cathode blower power reduction is largely due to the reduced airflow. The positive net reduction in blower power is further made possible by the mitigation of required blower pressure rise associated with eliminating the air preheater. Another benefit of cathode recycle is that it significantly increases the temperature level available for waste heat recovery (station 11); in this case by almost 600°C. System electric efficiency is improved to 31.8% and CHP efficiency to 60.2%.

3.2 Baseline Methane-Fueled SOFC-CHP System Description. The "baseline" design case for this study is a methane-fueled SOFC system (Case 2a) with heat recovery operating near atmospheric pressure with 100% external reforming as shown in Fig. 1. In this configuration, a waste heat boiler provides superheated steam at 5 bars and at a steam-to-carbon ratio of 2:1 for the external reformer. The boiler is located immediately downstream of the fuel reformer to ensure that a pinch temperature of 17°C or greater [26] is achieved. Air delivered to the system is preheated to 723°C before delivery to the cathode compartment of the cell-stack. The SOFC module operates at a nominal temperature of 800°C and 0.70 V/cell to produce 1.9 kW of dc power. The air blower consumes about 0.50 kW to supply the cooling air at 315 mbars, and 1.235 kW net ac power is generated at an overall system HHV efficiency of 33.6% (37.3%-LHV). Approximately 330 W of heat is rejected from the insulated hot zone of

the system, effectively reducing the combustor exit temperature below its adiabatic value. A large fraction of the thermal energy in the combusted product gas is required for the fuel processing reactions in the reformer. After the air preheater, the low-grade heat (~100°C) is further cooled to about 51°C in the hot water heating system to provide 0.63 kW of 60°C water. The system is capable of an overall cogeneration efficiency of only 50.6% (57%-LHV). Note that the efficiency of the baseline system configuration operating on methane fuel with an external steam reformer exceeds that of the hydrogen-fueled SOFC system, even though the hydrogen supplied to Case 1 was energetically "free." The performance advantage is due to the use of high grade thermal energy to steam reform the fuel and, thereby, liberate or produce additional hydrogen for electrochemical oxidation from the supply of water to the system [12].

Case 2b employs 100% internal reforming, respectively, and performance summary data can be found in Table 2. As the amount of internal reforming increases, the system airflow and blower parasitic power reduce allowing electric efficiency performance to reach 41.1% (45.6%-LHV) and CHP efficiency to 55.9% (62.4%-LHV). Cell power density is diminished by about 6% going from 0.407 W/cm^2 to 0.388 W/cm^2.

3.3 Methane-Fueled SOFC-CHP System With CGR. Cathode gas recycle as a system concept offers the advantage of reducing the size of the air preheater and blower components; thereby, reducing the system cost and increasing the temperature level of the exhaust gas stream that is available for thermal energy recovery. The system configuration of Case 3 is nearly identical to that of Case 2 shown in Fig. 1 with the exception that the boiler is preferentially located after the air preheater rather than before it, and an ejector (with recycle loop) is placed immediately downstream of the air preheater (see Fig. 2, for example) and operates with the same ejector efficiency of 20% as the hydrogen system. A comparison of the baseline system (Case 2a) and Case 3a reveals that airflow and parasitic power are reduced, and system electric efficiency is increased by 2% and CHP efficiency by 14%.

The TER of Case 3a also increases from 0.51 to 0.65. The addition of internal reforming and cathode gas recycle in the system concept of Case 3b enables an electric efficiency of nearly 42% to be achieved through large reduction in system airflow, but lowers the amount of thermal energy recovered as the change in

---

[1]Ejector efficiency is defined as $\eta_{ejector} = (\dot{V}_2/\dot{V}_1) \cdot (P_2 \cdot \ln(P_3/P_2)/(P_1-P_3))$ where $\dot{V}$ is the volumetric flow rate and P is the static pressure at the denoted location in the ejector. Subscripts 1, 2, and 3 refer to the primary driving flow (fresh air), the secondary flow (recycle), and the mixed flow at the ejector outlet, respectively.

TER from 0.65 to 0.21 shows. The increase in electric efficiency also results in a system heat loss of only 265 W—a reduction of about 20% from the baseline system. The combined effects of oxygen dilution on the cathode side and 100% internal reforming on the anode side of the SOFC serve to reduce cell-stack power density by almost 20% from the baseline system configuration.

Case 4b combines 100% internal reforming with anode gas recycle and improves the system electric efficiency by nearly 9% over Case 4a and the CHP efficiency is raised to 66.6% as a result of the reduced cooling airflow and associated parasitic power. A 68% reduction in the required cooling airflow is obtained by virtue of adding internal reforming into the system operation; the airflow reduction also reduces the system TER by 35%. Detailed process flowsheet parameters for Case 4b system configuration are provided in Fig. 3.

3.4 Methane-Fueled SOFC-CHP System With Internal Reforming and Cathode and Anode Gas Recycles. Case 5 depicted in Fig. 3 was the final system configuration studied and combines internal reforming, anode recycle (62% by mass), and cathode recycle (77% by mass). Significant system simplification is achieved with the incorporation of these system concepts, and Table 2 shows that at 1.235 kW net power output, an electric efficiency of 41.4% (45.9%-LHV), a CHP efficiency of 70.0%, and a TER of 0.69 are achieved. System heat loss from the hardware hot zone is minimized to less than 270 W. The combined effects of internal reforming and recycle of depleted electrode gases result in a lower SOFC stack power density (0.35 W/cm^2) than Cases 2 and 4. However, the use of anode gas recycle mitigates the reduction in stack power density normally associated with internal reforming operation as evidenced in a comparison of Cases 2a and 2b.

3.5 Establishing an Optimal SOFC-CHP System Configuration. The analysis of the various system configurations indicates that systems incorporating internal reforming provide the highest electric efficiency, while those also utilizing SOFC exhaust gas recycle increase the system TER to improve the match with residential domestic hot water requirements in U.S. households. While energetic performance analysis of the system configurations given in Cases 1–5 is insightful, by itself, it is insufficient in distinguishing between preferred system designs. Life-cycle cost estimation is far more revealing in terms of establishing optimal configurations and identifying key parameter sensitivities.

Although the cost-of-electricity as given in Eqs. (1) and (4) amortizes the capital and maintenance costs of the power generator over its life, the metric is more representative of the equivalent electricity price to be charged over a specified period of time, such as winter or summer season. In contrast, the life-cycle costs as given by Eqs. (6)–(8) estimate the net present worth of capital and operating costs over the life of the system. Reference economic parameters utilized in the cost estimation are summarized in Table 3, and the normalized capital cost, cost-of-electricity, and life-cycle costs for each of the system configurations are plotted in Figs. 4 and 5. Figure 4 shows that internal reforming-based systems offer the lowest capital cost, and the addition of waste heat recovery hardware and control can add over 20% to the capital cost. Hydrogen-fueled systems are lower in capital cost (by as much as 45%) as expected given the reduced number of system components (see inset of Fig. 4). This plot also shows that capital cost comparisons are not particularly revealing in terms of system differentiation as the internal reforming Cases 2b, 3b, 4b, and 5 have similar expected costs.

The normalized cost-of-electricity plot of Fig. 5(a) reveals that from a third party owner perspective, systems with anode gas recycle and internal reforming offer the lowest CHP-based COE compared with the baseline configuration. Interestingly, the value of the recovered heat varies for each system and is found to be

Table 3 Summary of technical and economic parameters employed in analysis

Parameter	Value
Production volume (units/year)	50,000
Natural gas price ($/therm)	1.0
Electricity price ($/kWh)	0.104
Electric capacity factor (%)	90
Plant availability (%)	99.5
Electric price inflation rate, i_{infl} (%)	2.2
Natural gas price inflation rate, i_{infl} (%)	5.0
Equipment price inflation rate, $i_{g,infl}$ (%)	2.59
SOFC stack life (year)	5
SOFC salvage value at the end-of-life (%)	10
Average hourly domestic hot water load (kW$_{th}$)	1.1
Average hourly electric load (kW)	1.0
Conventional hot water heater efficiency (%-HHV)	60
Fuel cell design power (kW)	1.235
SOFC nominal voltage (V/cell)	0.70
SOFC fuel utilization (%)	85
SOFC nominal cell temperature (°C)	800

negative[2] in cases involving internal reforming without anode gas recycle (Cases 2b and 3b). In these cases, the increase in system capital and maintenance cost cannot be successfully overcome by the gain in CHP efficiency. The value of the waste heat ranges from –$0.005/kWh to $0.035/kWh. In contrast, due to the high fuel cost of hydrogen, systems utilizing hydrogen as a fuel (Case 1) experience COEs that are up to 80% higher than the baseline electric-only system. The COE penalty for hydrogen-fueled SOFC-CHP systems is only 10–20% above the baseline CHP case configuration. However, it should be noted that this result is due in part to the fact that the CHP-based COE estimate assumes that hydrogen also fuels the domestic hot water heater. Clearly conclusions drawn from cost comparisons between hydrogen-fueled and methane-fueled systems are suspect as the relative fuel costs for either system are highly uncertain and depend on projections that may be decades in the future. Nevertheless, were hydrogen-based systems to be installed in the near future with access to fuel delivery at prices targeted by DOE ($\sim$$3.30/kg$_{H_2}$), sizable energy cost increases over natural gas would be expected without incentives.

The plots of normalized life-cycle costs of the various system configurations in Fig. 5(b) demonstrate a very similar trend as the plot for COE. One prime difference between these two metrics is that LCC analysis shows that CHP-systems offer reduced costs from electric-only systems in all cases. This advantage arises from the offset fuel costs that are realized as a result of on-site cogeneration. As with COE-based analysis, systems incorporating both anode recycle and internal reforming offer the lowest life-cycle cost due to efficiency improvements and first cost reductions. In general, life-cycle costs are up to 30% lower for CHP-systems than electric-only based configurations due to the value of the waste heat recovery that offsets utility gas consumption.

Breakdowns of the contributions of fuel, operation and maintenance (O&M), and capital to the total COE and LCC objective functions are shown in Fig. 6. For life-cycle costs, the O&M costs are estimated as a function of the first costs of the system and are included in the capital cost segment of the bar plot. Additionally, since these cost analyses are for grid-connected systems, some amount of electricity and fuel is purchased from the utility to meet the total energy demand of the residence. These contributions are only relevant for the LCC function and are denoted by "U. Electric" and "U.Fuel." The portion of the life-cycle cost used to supply fuel to the fuel cell system is denoted as "FC Fuel." Over half of the cost-of-electricity for the baseline case as shown in Fig.

_____

[2]The value of heat is estimated as the difference between COE$_{eo}$−COE$_{CHP}$.
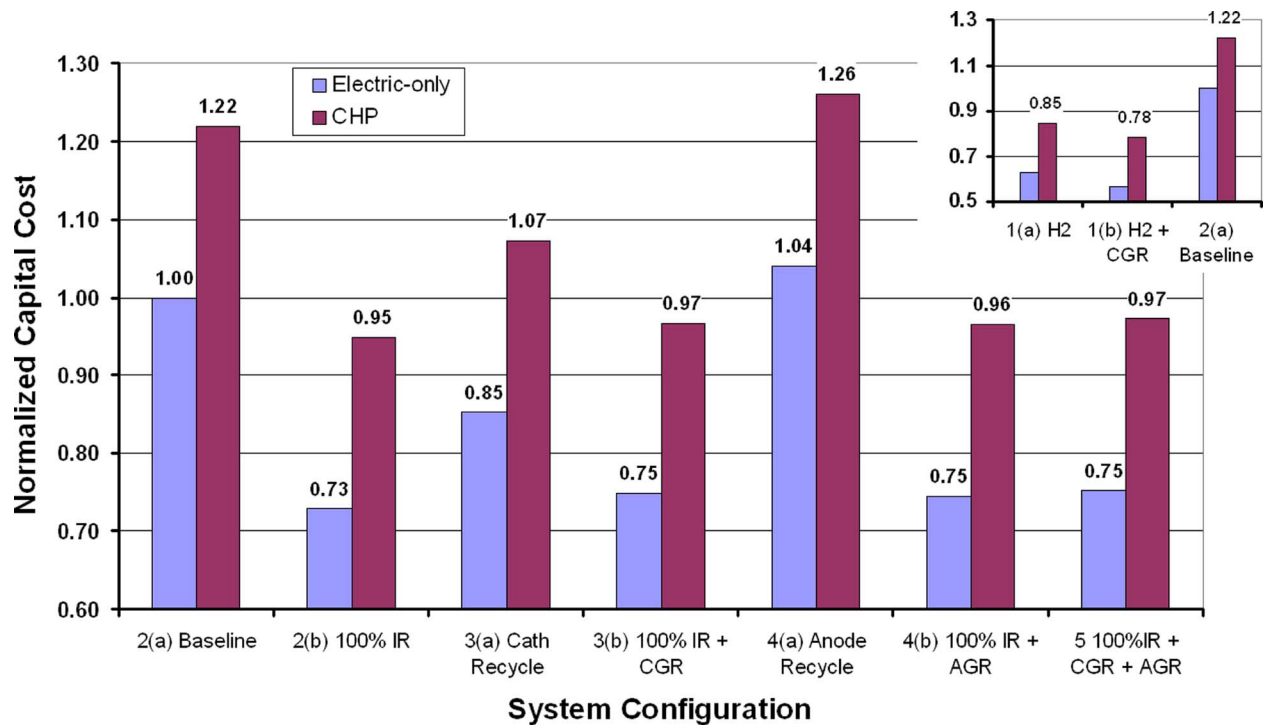
Fig. 4 Normalized capital cost for each system configuration

$6(a)$ is influenced by the fuel cost to operate the SOFC system. When the value of the waste heat recovered for domestic hot water usage is accounted for, the fuel portion of the COE is reduced, but still represents half of the total. O&M cost contributes less than 15% of the total COE. A breakdown of the LCC contributions indicates a similar trend as that of the COE. As Fig. $6(b)$ shows, the relative breakdowns of COE and LCC contributions are not significantly changed by moving to an optimal system configuration such as that given by Case 5, despite life-cycle cost reductions of up to 30%.

Given the uncertainty of relative cost estimates (5–10%) between system configurations, neither COE nor LCC analyses clearly identify an optimal configuration among Cases 3b, 4b, and 5. A closer examination at these three potential system configurations using LCS (see Eq. (6)) is shown in the bar plot of Fig. 7. When normalizing the life-cycle savings to that of the Case 3b system configuration, Case 4b obtains an increase of over 50% in life-cycle savings and Case 5 achieves an increase of over 80%. This comparison suggests that Case 5 offers the most optimal life-cycle benefits relative to other system configurations and that the intersection of both high efficiency and lowest cost can be obtained. In addition to life-cycle economic benefits, it is also useful to balance these results against a qualitative understanding of the technical risks and uncertainties in system design.

3.6 Additional Considerations in Optimal System Design. The viability of the various system configurations is also dependent on the hardware availability, durability, and control complexity. For example, in practice, the use of a gas ejector for recycle of cathode gases can be problematic to implement due to poor controllability of the amount of recycle throughout the operating envelope. Off-design operability may also require a small air preheater to ensure air temperature control at the stack inlet if recycle performance is poor. As has been previously reported [12], systems incorporating high temperature recycle blowers would accomplish much of the same effect as that of an ejector through the reduction in air preheater duty and reduced overall parasitic power. While high temperature recycle blowers are another possible consideration for use in SOFC systems, the service tempera-

ture requirements are severe and capital and maintenance cost increases can be substantial [32]. Furthermore, reliability is critical in residential power systems and additional risks with BOP hardware still under development should be minimized. Considerations of control complexity, reliability, and cost risk tend to mitigate the calculated benefits of a Case 5 system configuration. Thus, the system design of Case 4b is explored further in terms of optimal operating parameter selection using life-cycle cost minimization.

4 Selection of Optimal SOFC Operating Parameters

SOFC stack operating parameters of interest include nominal cell voltage, fuel utilization, cell temperature, and allowable cathode air temperature rise. Optimal selection of each of these parameters involves observing constraints, such as minimum airflow requirements (i.e., $\lambda \geq 1$), and recognition that these parameters are not independent of one another. Additional considerations involve the practical realities of the relationships between cell life/durability and these parameters.

4.1 Optimal Cell Voltage and Fuel Utilization. The influence of a variation in cell voltage and fuel utilization on system efficiency and the number of cells in the SOFC stack required to meet the 1.235 kW net ac power load is shown in Fig. $8(a)$. As the nominal cell voltage is increased in the Case 4b system configuration, system efficiency increases and cell power density is lowered. Over the range of cell voltage explored, the system efficiency increases from 31%- to 51%-HHV, and the number of cells in the SOFC stack increases by over 300%. The implications of these trends in terms of normalized life-cycle costs for both electric-only and CHP-systems are explored in the plots depicted in Fig. $8(b)$. Life-cycle fuel costs are reduced with increasing cell voltage by an amount greater than incremental increases in system first costs associated with the fuel cell-stack. This trend continues until the increase in the capital cost due to the increasing number of cells in the stack to produce the required amount of power (i.e., cell power density) offsets the efficiency gains. For fuel utilizations of 85%, optimum cell voltages are observed at 0.685 V and
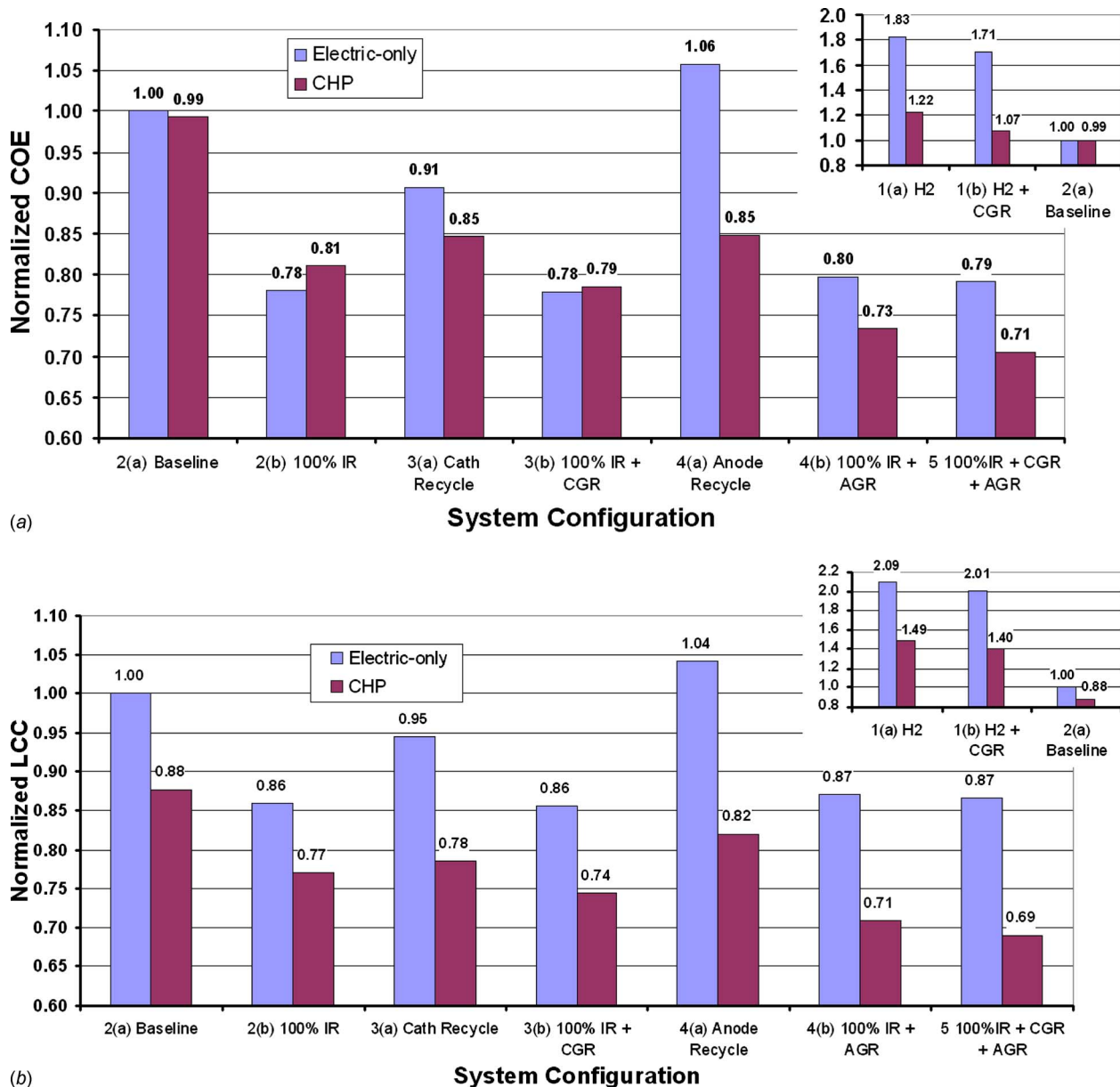
Fig. 5 Normalized cost-of-electricity and life-cycle cost for each system configuration: (a) normalized COE and (b) normalized LCC

0.76 V for CHP and electric-only systems, respectively. As Fig. 8(b) shows, The CHP-configuration demonstrates a 1–12% lower life-cycle cost depending on selection of cell voltage. When system fuel utilization is decreased from 85% to 75%, life-cycle costs increase throughout the voltage range for the electric-only system, as lowering fuel utilization not only increases cell power density (reduces capital cost) but also reduces system efficiency. In the case of CHP-configurations, the reduction in electric efficiency due to lower fuel utilization can be offset by the increase in waste heat recovery so that a fuel utilization of 75% ultimately yields the lowest LCC at a cell voltage of 0.75 V. Simultaneous exploration of the cell voltage and fuel utilization parameter space indicates that a global optimum is likely at 0.75 V and 75% fuel utilization for the Case 4b system operating with the settings given in Table 3. For systems intended for electric-only applications, the minimum LCC favors higher design point cell voltage and higher fuel utilizations, while a balance is struck between voltage and fuel utilization for CHP-systems.

4.2 Optimal Cell Temperature and Air Temperature Rise.
Increasing cell operating temperature reduces the cell polarizations and results in improved efficiency performance as Fig. 9(a) shows. The cost model incorporates the change in SOFC stack and air recuperator material requirements as operating temperature is altered up or down from its nominal value of 800°C and the cell model responds to changes in cell resistance due to changes in operating temperature. Figure 9(a) illustrates that as the nominal cell operating temperature is increased from 700°C to 850°C, the normalized LCC is decreased by as much as 10%. This figure also shows the sensitivity of LCC to changes in cell voltage and temperature. When the operating voltage is increased from its baseline value of 0.7 V/cell to 0.75 V/cell at a given temperature, the LCC is reduced. This characteristic is largely due to the benefits of reduced fuel costs from increased operating efficiency. Furthermore, capital cost increases with higher operating temperature can be mitigated or even reduced as second order effects such as re-
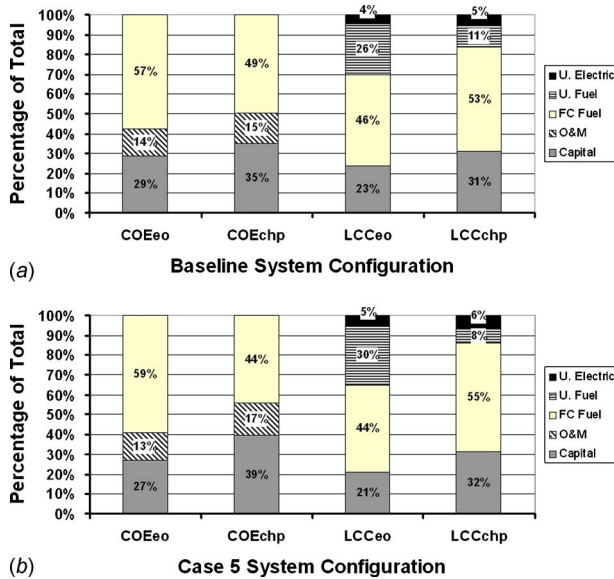
Fig. 6 Breakdown of life-cycle cost contributions: (*a*) **Case 2a cost breakdown and** (*b*) **Case 5 cost breakdown**

duced airflow, and, therefore, reduced air preheater duty and cost compensate for higher SOFC capital costs. However, Fig. 9(*a*) reveals that the benefits of selecting a higher design cell voltage diminish with increasing operating temperature as gains in cell efficiency and airflow reduction are nonlinear and are ultimately
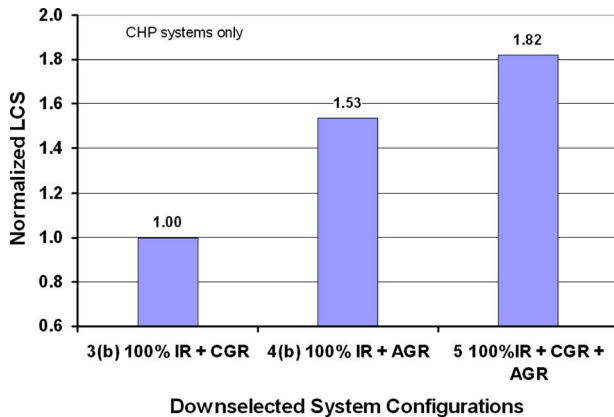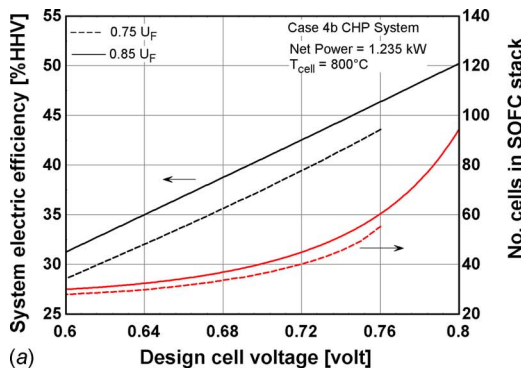

Fig. 7 Normalized life-cycle savings versus system configuration

Fig. 8 The effect of cell voltage on normalized LCC, system efficiency, and stack size: (*a*) **system efficiency and number of cells in SOFC stack, and** (*b*) **normalized LCC**

bounded by the minimum system airflow requirements.

The variation of life-cycle costs is also analyzed for changes in design air temperature rise across the cathode. This analysis assumes that it is possible to achieve acceptable levels of thermally induced internal cell stresses due to the increased cell temperature gradient via stack and/or cell design strategy. The plots in Fig. 9(*b*) are generated by maintaining the nominal cell operating temperature at 800°C, but altering the allowable cathode air temperature rise across the cell. An increase in cell temperature rise from 75°C to 200°C reduces the LCC metric by 4% for a nominal 0.7 V/cell condition and by less than 2% for a 0.75 V/cell operating point. It is further observed that the use of 100% internal reforming and operation at higher cell voltages leads to LCC optima constrained by minimum airflow requirements. Figure 9 shows that, in general, the opportunity to reduce LCC of the system design is greater for increases in cell operating temperature than for increasing the allowable air temperature rise.

4.3 Global Optima. Locating the minimum CHP LCC for Case 4b system configuration involved a comprehensive parametric analysis that constrained optima to system airflows with stoichiometric ratios of at least 1.4 (i.e., $\lambda \geq 1.4$). This value of excess air is somewhat arbitrary but is intended to provide design margin, allowing for changes in airflow requirements as the cell-stack voltage decays over its life. Parametric optimization over the parameter space of 0.6 V/cell to 0.8 V/cell, 69% to 92% fuel utilization, 700°C to 850°C cell temperature, and 75°C to 200°C air temperature rise reveals several LCC optima within less than 2% of each other. The global minimum was found at 0.7 V/cell, $0.75 U_f$, 850°C cell temperature, and 175°C cathode air temperature rise. At these operating conditions, the system LCC (=0.673) is reduced by about 33% below the baseline system configuration value. System electric efficiency performance is about 40% and CHP efficiency is 69% at these SOFC parameter settings, and the required cell power density is 0.42 W/cm² with a minimized stoichiometric airflow of $\lambda = 1.4$. The analysis results suggest that the optima are driven toward solutions that maximize cell temperature and air temperature rise, minimize cell voltage and fuel utilization, and approach or reside at the constraint of minimum airflow. Within a given material temperature range, maximizing cell temperature achieves increases in system efficiency, cell power density, and a decrease in SOFC capital cost. Increasing the cathode air temperature rise lowers BOP capital cost and increases system efficiency through reductions in air blower parasitic power, but in increments that are smaller than those gained by elevation of cell temperature. Reduction in cell voltage and, hence, system efficiency (see Fig. 8(*b*)) can be overcome by increases in cell temperature and allowable air temperature rise. These observations indicate that the optimal values of LCC are achieved by maximizing system efficiency and minimiz-
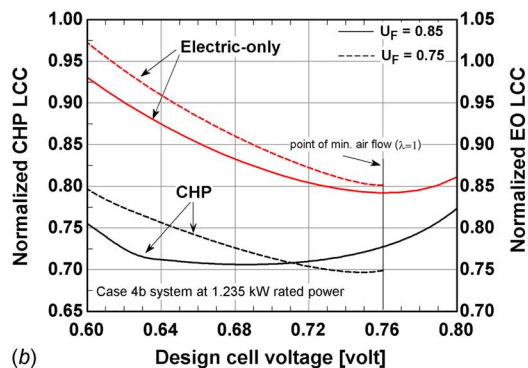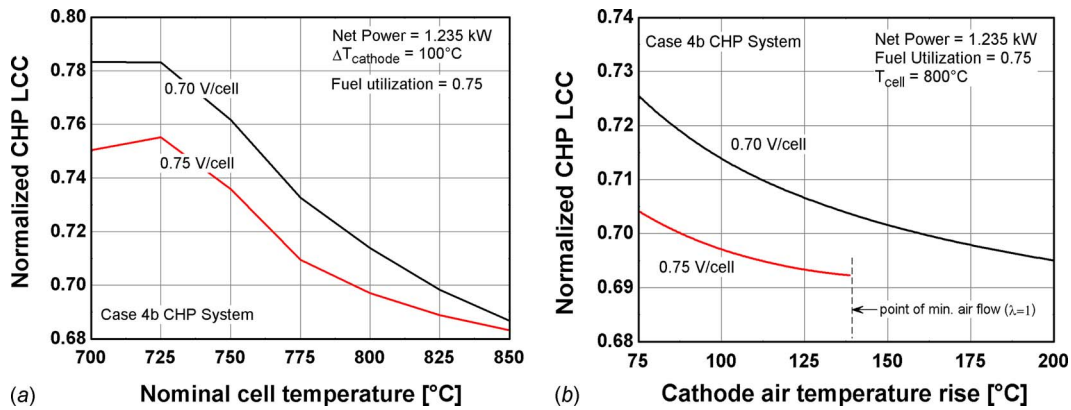
Fig. 9 The effect of cell temperature and air temperature rise on normalized SOFC-CHP LCC: (a) LCC versus cell temperature and (b) LCC versus cathode air temperature rise

ing the number of cells in the stack (the highest capital cost component) until parameter constraints in cell temperature, $\Delta T_{cathode}$, or λ_{air} are reached.

Practical considerations in selection of SOFC design parameters are heavily influenced by cell life and durability. Raising cell temperatures and lowering design voltages (increasing current density) generally reduce cell life [36]. Furthermore, a 40,000 h SOFC stack with an average voltage degradation rate of 0.5%/1000 h will decay on the order of 160 mV/cell from beginning-of-life to end-of-life. Thus, end-of-life current densities must be higher to satisfy the same power demand at the beginning-of-life. The systems-level perspective must account for the increased reactant flows at the end-of-life and this may ultimately provide little leeway in the selection of cell voltage. For the purposes of this analysis, it is insightful to quantify the benefits without such restrictions by assuming that cell voltage parameter exploration is essentially one of the median cell voltage design conditions (i.e., middle-of-life performance).

5 Additional Considerations for Optimal Design of SOFCs in Residential Applications

A comparison of the normalized life-cycle costs for all of the system configurations given in Table 2 with a conventional residential energy system that supplies heat and power by a natural

gas-fired water heater and utility grid power, respectively, is presented in Fig. 10. The LCCs are normalized to the conventional system for production volumes of 50,000 units/year, and the results show that only the optimized SOFC-CHP system achieves life-cycle costs lower than the conventional system at the ~1.2 kW scale. As the figure illustrates, residential SOFC systems can be cost competitive in a business-as-usual economic environment only when the system design is properly optimized. It is also important to recognize that these results employ national average utility pricing, and, therefore, the economic viability of SOFC-CHP systems at this scale has a geographic dependence. The techno-economic optimal system design is influenced by the economies of production and scale. The sensitivity of the system LCC and LCS to these variables is explored next.

5.1 Sensitivity of LCC to Economy of Production and Scale. The variation of life-cycle cost with changes in production volume is depicted in Fig. 11(a). It is interesting to note that by increasing the production rate from the base case of 50,000 units/year to 1×10^6 units/year, the 25% reduction in capital cost that is achieved translates into a life-cycle cost reduction of only 6%. In a similar fashion, Fig. 11(b) illustrates that the economy of scale in moving from a 1 kW SOFC-CHP system to a 10 kW system produces a decrease in system capital cost of 40%, but yields only a 10% decrease in life-cycle costs (assuming an
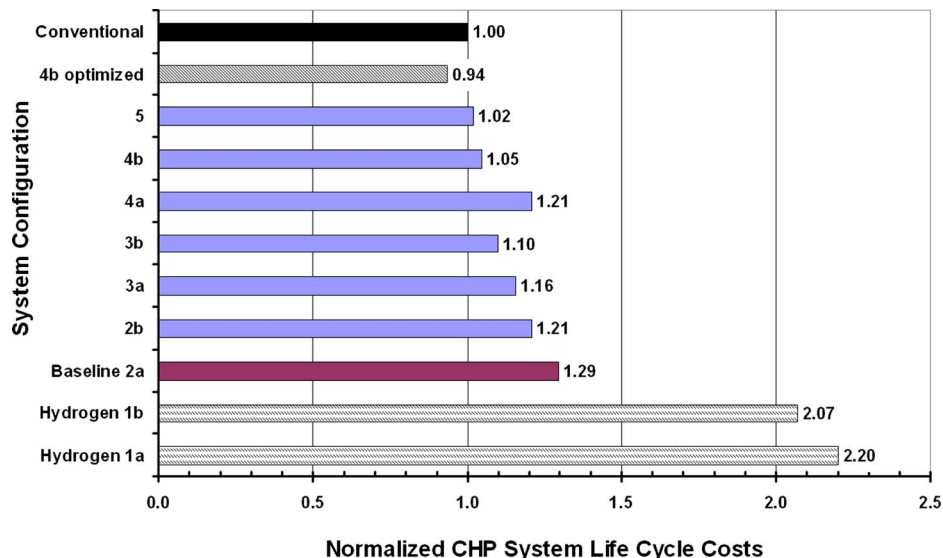

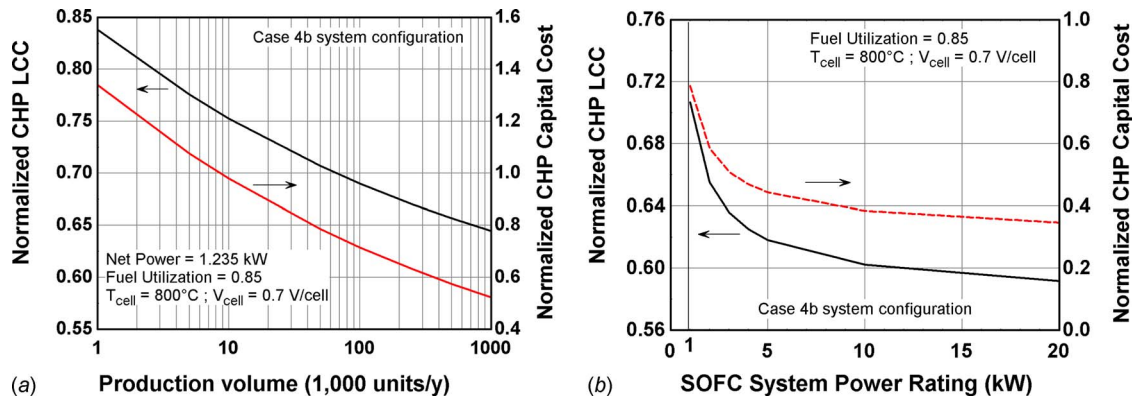**Fig. 10 Comparison of SOFC-CHP and conventional system life-cycle costs**

Fig. 11 Sensitivity of normalized life-cycle and capital costs to production volume and system size: (*a*) LCC sensitivity to production volume and (*b*) LCC sensitivity to power rating

equivalent ten times increase in thermal and electric loads by the application). Thus, the net effect of capital cost reduction in life-cycle costs follows an approximate ratio of 4:1. The characteristic of system power rating versus capital cost shown in Fig. 11(*b*) suggests that preferred system capacities are at least 10 kW in size. Additionally, while not shown, the large reduction in capital cost with increasing system size also produces significant gains in system life-cycle savings.

5.2 Life-Cycle Savings. The techno-economic performance of all the ~1.2 kW system configurations analyzed (Cases 1–5) operating under the parameters summarized in Table 3 yields negative life-cycle savings (see Fig. 10). The optimal configuration and parameter selection achieve positive life-cycle savings, although only marginally so for the average utility pricing given in Table 3. As system power rating increases, the life-cycle savings increase in a proportion that is significantly greater than the change in system size. For example, the life-cycle savings of serving a 2 kW household with a nonoptimized Case 4b system configuration with anode gas recycle operating at 90% capacity factor is estimated to be $960; or alternatively, a unit life-cycle savings of $480/kW of system capacity. Assuming the same capacity factor for a 20 kW system, the unit life-cycle savings reach a value of about $1800/kW of power delivered. Thus, the life-cycle savings benefit of larger systems further supports the conclusion of increasing SOFC-CHP system size to target application in multifamily dwellings rather than single-family residences.

6 Conclusions

The techno-economic optimal design study was carried out through a comprehensive parametric analysis employing detailed system, component, and cost models. Optimal system configurations for application in residential dwellings were identified using life-cycle cost objective functions, and the economic differentiation between system designs was quantified to within a satisfactory degree of resolution/uncertainty. The value of the waste heat was also found to vary from configuration to configuration and ranged from −$0.005/kWh to $0.035/kWh. Systems with waste heat recovery achieved lower life-cycle costs than their electric-only counterpart in an amount that ranged from 9% to 23%. System configurations characterized by both high efficiency and low capital and life-cycle cost were found to be possible and not mutually exclusive. The optimal system configuration was one that included anode and cathode gas recycles and 100% internal reforming. However, the Case 4b system configuration did not use cathode gas recycle and was considered for further optimization after considerations involving system control, operability, and overall technical risk.

Optimal SOFC operating parameter selection was also examined using LCC minimization on the Case 4b system configura-

tion. Different optimum cell voltages were observed for electric-only systems versus CHP-systems. Electric-only systems typically favored higher cell voltage and higher fuel utilization design points. Lower fuel utilization (75% versus 85%) is desirable for micro-CHP systems, and the reduced electric efficiency is compensated by the waste heat recovered and the reduced parasitic from higher fuel cell efficiency and lower electrochemical heat release. However, reducing fuel utilization beneath 75% is constrained by satisfying minimum system stoichiometric airflow requirements. Finally, the benefit of economy of scale in terms of life-cycle savings strongly suggests that SOFC-CHP systems be applied in multifamily residential settings in the 10–20 kW size range.

Acknowledgment

Nomenclature

A = plant availability
ac = ac power
C = unit cost, $/kW
CF = capacity factor
COE = cost-of-electricity, $/kWh
dc = direct current power
ER = external reforming
F = first year operating cost
F_C = unit fuel cost, $/therm
F_H = fraction of utilizable thermal energy from fuel cell
HHV = higher heating value, J/mol
i = inflation rate
k = unit conversion constant
LCC = life-cycle cost
LHV = lower heating value, J/mol
MC = levelized annual maintenance cost, $/kWh
$\dot{m}$ = mass flow rate, g/s
$\dot{n}$ = molar flow rate, mol/s
P = present worth factor; pressure; annual electricity price, $/kWh
$\dot{Q}$ = thermal energy flow rate, W
R_F = capital recovery factor
S = equipment size
T = temperature, °C
U_F = fuel utilization
UA = heat exchanger performance characteristic
V = cell voltage; production volume

$\dot{V}$ = volumetric flow rate

$\dot{W}$ = rate of work production or electric power

Greek Letters

Δ = change in

ε_H = heating or thermal energy recovery efficiency

η = efficiency

λ = amount of excess air

ξ = extent of reaction conversion

Subscripts/Superscripts

e, elec = electric

eo = electric-only

f = fuel

h, htg = heating

infl = inflation

j = component index

prod = production

rec = recovered

ref = reference

sys = system

th = thermal

References

[1] Energy Information Administration, 2002, "Table 2.1a Energy Consumption by Sector, 1949–2002," Annual Energy Review.

[2] Energy Information Administration, 2002, "Table 2.6 Household Energy Consumption and Expenditures by End Use and Energy Source, Selected Years, 1978–1997," Annual Energy Review.

[3] Kreutz, T. G., and Ogden, J. M., 2000, "Assessment of Hydrogen-Fueled PEM Fuel Cells for Distributed Generation and Cogeneration," *Proceedings of the 2000 U.S. DOE Hydrogen Program Review*, Report No. NREL/CP-570-28890.

[4] Gunes, M. B., and Ellis, M. W., 2003, "Evaluation of Energy, Environmental, and Economic Characteristics of Fuel Cell Combined Heat and Power Systems for Residential Applications," ASME J. Energy Resour. Technol., **125**, pp. 208–220.

[5] Marechal, F., Palazzi, F., Godat, J., and Favrat, D., 2005, "Thermo-Economic Modelling and Optimisation of Fuel Cell Systems," Fuel Cells, **5**(1), pp. 5–24.

[6] Khandkar, A., Hartvigsen, J., and Elangovan, S., 2000, "A Techno-Economic Model for SOFC Power Systems," Solid State Ionics, **135**, pp. 325–330.

[7] Baratto, F., Diwekar, U. M., and Manca, D., 2005, "Impacts Assessment and Trade-Offs of Fuel Cell-Based Auxiliary Power Units: Part I. System Performance and Cost Modeling," J. Power Sources, **139**, pp. 205–213.

[8] Baratto, F., Diwekar, U. M., and Manca, D., 2005, "Impacts Assessment and Trade-Offs of Fuel Cell Based Auxiliary Power Units: Part II. Environmental and Health Impacts, LCA, and Multi-Objective Optimization," J. Power Sources, **139**, pp. 214–222.

[9] Hawkes, A., Aguiar, P., Hernandez-Aramburo, C., Leach, M., Brandon, N., Green, T., and Adjiman, C., 2006, "Techno-Economic Modelling of a Solid Oxide Fuel Cell Stack for Micro Combined Heat and Power," J. Power Sources, **156**, pp. 321–333.

[10] Hawkes, A., and Leach, M., 2005, "Solid Oxide Fuel Cell Systems for Residential Micro-Combined Heat and Power in the UK: Key Economic Drives," J. Power Sources, **149**, pp. 72–83.

[11] Alanne, K., Saari, A., Ugursal, V., and Good, J., 2006, "The Financial Viability of an SOFC Cogeneration System in Single-Family Dwellings," J. Power Sources, **158**, pp. 403–416.

[12] Braun, R. J., Klein, S. A., and Reindl, D. T., 2006, "Evaluation of System Configurations for Solid Oxide Fuel Cell-Based Micro-Combined Heat and Power Generators in Residential Applications," J. Power Sources, **158**, pp. 1290–1305.

[13] Braun, R. J., 2002, "Optimal Design and Operation of Solid Oxide Fuel Cell Systems for Small-Scale Stationary Applications," Ph.D. thesis, University of Wisconsin-Madison, Madison, WI.

[14] Braun, R. J., Klein, S. A., and Reindl, D. T., 2004, "Considerations in the Design and Application of Solid Oxide Fuel Cell Energy Systems in Residential Markets," ASHRAE Trans., **110**.

[15] Exeltech, 2000, MX Series product brochure, Fort Worth, TX, www.exeltech-.com.

[16] Engineering Equation Software (EES), 2005, F-Chart Software, Middleton, WI, www.fchart.com.

[17] Ellis, M. W., and Gunes, M. B., 2002, "Status of Fuel Cell Systems for Combined Heat and Power Applications in Buildings," ASHRAE Trans., **108**.

[18] Duffie, J. A., and Beckman, W. A., 1991, *Solar Engineering of Thermal Processes*, 2nd ed., Wiley Interscience, New York.

[19] Starrs, T. J., 2000, "Summary of State Net Metering Programs," Kelso Starrs & Associates, LLC, Feb.

[20] Alderfer, R. B., Eldridge, M. M., and Starrs, T. J., 2000, "Making Connections: Case Studies of Interconnections and Their Impact on Distributed Power Projects," National Renewable Energy Laboratory, Report No. NREL/SR-200-28053.

[21] Myers, D. B., Ariff, G. D., James, B. D., Lettow, J. S., Thomas, C. E., Kuhn, R. C., 2002, "Cost and Performance Comparison of Stationary Hydrogen Fueling Appliances," Task 2 report prepared for the U.S. DOE under Grant No. DE-FG01-99EE35099.

[22] Energy Information Administration, 2008, "Average Retail Price of Electricity to Ultimate Customers by End-Use Sector, 1995 Through 2006," Table 7.4, Electric Power Annual Data.

[23] Mugerwa, M. N., and Blomen, L. J., 1993, "Fuel Cell System Economics" *Fuel Cell Systems*, L. J. L. Blomen and M. N. Mugerwa, eds., Plenum, New York.

[24] Arthur D. Little, llc, 2001, "Conceptual Design of POX/SOFC 5 kW Net System," final report, prepared for the U.S. Department of Energy, National Energy Technology Laboratory.

[25] Thijssen, J. H., 2007, "The Impact of Scale-Up and Production Volume on SOFC Manufacturing Cost," final report, prepared for the U.S. Department of Energy, National Energy Technology Laboratory.

[26] Lundburg, W. L., 1989, "Solid Oxide Fuel Cell Cogeneration System Conceptual Design," final report, prepared for the Gas Research Institute (GRI), Report No. GRI-89/0162.

[27] Itoh, H., Mori, M., Mori, N., and Abe, T., 1994, "Production Cost Estimation of Solid Oxide Fuel Cells," J. Power Sources, **49**, pp. 315–332.

[28] Krist, K., Wright, J. D., and Romero, C., 1995, "Manufacturing Costs for Planar Solid Oxide Fuel Cells," *Proceedings of the Fourth International Symposium on Solid Oxide Fuel Cells*, The Electrochemical Society, Osaka, Japan, pp. 24–32.

[29] James, B. D., Lomax, F. D., and Thomas, C. E., 1999, "Manufacturing Cost of Stationary Polymer Electrolyte Membrane (PEM) Fuel Cell Systems," final report, prepared for the U.S. Department of Energy, National Renewable Energy Laboratory.

[30] Adame, B., 2008, Haynes International Inc., private communication.

[31] TIAX, llc, 2002, "Scale-Up Study of 5-kW SECA Modules to a 250 kW System," final report, prepared for the U.S. Department of Energy, National Energy Technology Laboratory.

[32] Johnson, M., 2006, Phoenix Analysis and Design Technologies, Inc., private communication.

[33] Polak, D. R., 2001, "A Thermoeconomic Model for Residential Fuel Cell Systems Studies," final report, United Technologies Research Center.

[34] Surdoval, W., 2006, "U.S. DOE Fossil Energy Fuel Cell Program Review," *Proceedings of the Seventh SECA Public Workshop and Peer Review*, Philadelphia, PA, Sept. 14–16.

[35] Doyon, J., 2006, "SECA SOFC Programs at Fuel Cell Energy, Inc.," *Proceedings of the Seventh SECA Public Workshop and Peer Review*, Philadelphia, PA, Sept. 14–16.

[36] Linderoth, S., and Mogensen, M., 2000, "Improving Durability of SOFC Stacks," *Proceedings of the Fourth European SOFC Forum*, Lucerne, Switzerland, Jul.